Effects on p-^{11}Li elastic scattering of core recoil and virtual 2-n halo breakup

R. Crespo*
Departamento de Física, Instituto Superior Técnico, Av Rovisco Pais, 1049-001 Lisboa, Portugal

I. J. Thompson†
Department of Physics, University of Surrey, Guildford, Surrey GU2 7XH, United Kingdom
(Received 10 March 2000; revised manuscript received 23 October 2000; published 6 March 2001)

We have evaluated the differential cross section for ^{11}Li scattering from protons at 800 MeV/nucleon using the single-scattering approximation to Kerman-McManus-Thaler multiple-scattering expansion of the optical potential, and also the multiple-scattering expansion of the total T matrix. Using the same projectile density distributions and nucleon-nucleon transition amplitudes as inputs, we show that the two scattering frameworks produce significantly different elastic-scattering observables. We also show that the predictions from the two approaches differ because of core recoil and virtual breakup of the valence halo neutrons, which tend to produce opposite effects.

DOI: 10.1103/PhysRevC.63.044003 PACS number(s): 24.10.Ht, 25.40.Cm

I. INTRODUCTION

Traditionally, the scattering of a proton from a stable nucleus has been reasonably well described by mean-field (MF) optical-model (OM) microscopic theories, for example, the multiple-scattering expansion of the optical potential, such as formulated by Kerman-McManus-Thaler (KMT) [1] or Watson [2], and the Glauber optical-model limit [4,5]. These formalisms rely on the validity of a mean-field description of the stable nuclei: all the nucleons are treated on an equal footing, and the nuclear structure information in the optical-potential operator is derived entirely from the total matter density. The G-matrix approach [3] starts with infinite nuclear matter and uses the local-density approximation to evaluate the optical potentials for finite nuclei, whereas in the other frameworks the finite aspects of the nuclei are taken into account from the onset. Mean-field optical model calculations have been performed within different scattering formalisms for elastic scattering of protons from helium isotopes [6–8] with good success in understanding experimental cross sections, and from lithium isotopes [9,10] with somewhat less success.

This range of success may be attributed to the fact that we know that there are some scattering observables for the elastic scattering of halo nuclei that depend on properties beyond that of the total density. For example, few-body structure models of light halo nuclei have been developed [11] to properly take into account the few-body degrees of freedom of a system of loosely bound valence nucleons orbiting around a relatively tightly bound core, for example in ^{11}Li. Then, on the reaction side, few-body Glauber and adiabatic theories [12–14] have been applied to study the scattering of halo nuclei from stable nuclei, and significant differences in elastic scattering systematically arise when compared with optical model limits. However, with these formalisms it is not possible to extract in a clear way how the halo density and cluster functions contribute to the scattering.

Recently, a multiple scattering expansion of the total transition amplitude (MST) was developed [15]. An advantage of this approach is that reaction mechanism and structure effects are now clearly delineated. It was shown in [15] that the relevant halo-structure information for the scattering is associated with the halo density, *together with* the density distribution for the core center-of-mass motion due to core-recoil effects. However, these pieces of halo-structure information do not combine in a way that contributes to the scattering as a total matter density. Thus, a few-body treatment of the reaction mechanism for halo-nuclei elastic scattering necessarily incorporates structure features that go beyond knowledge of the total-matter-density distribution alone. At intermediate and high energies these effects were found to produce significant differences in the calculated elastic scattering [15].

A full *understanding* of reaction theory at the intermediate and high-energy region has not, to date, been satisfactorily achieved. With respect to scattering involving stable nuclei within a nonrelativistic framework, the G-matrix method is able to give a fairly good description of the elastic data while including Pauli blocking effects. An independent analysis within the KMT approach [16] has shown, however, that these higher order Pauli blocking effects are very small, and this apparent discrepancy has remained an open problem. With respect to scattering involving halo nuclei, the G-matrix approach has proved to give a reasonable description of the elastic data for proton scattering from halo nuclei at intermediate energies. On the other hand, the single-scattering approximation of the KMT optical-model framework described in a satisfactory way a ''skin'' nucleus ^{8}He [6], but has failed to reproduce the case of proton scattering from ^{11}Li [9] at similar energies. In parallel to this, few-body theories have been developed on Glauber [12,13] and other [14] bases, and applied to study the scattering involving halo nuclei in the high-energy regime. To help establish which scattering theory should be used in the case of halo nuclei, our aim is to isolate some relevant physics that needs to be

*Email address: raquel@wotan.ist.utl.pt
†Email address: I.Thompson@surrey.ac.uk

incorporated into the theory at the high-energy regime under consideration.

To get insight into some of these theoretical issues, in this paper we compare the results of the KMT MF optical model and the MST few-body scattering formalisms in the high-energy regime, making use of the *same halo structure* and the *same* dynamical information. This comparison will provide a framework to disentangle aspects of physics related to the few-body dynamical treatment of halo nuclei, aspects that will be probed when there are accurate data with small error bars. In our comparison, both formalisms will have as structure input the density distributions for the core, the valence nucleons, and the core center-of-mass motion. For simplicity, we make use of a simple structure-cluster model [17]. We have here in mind ^{11}Li, which will be assumed to be described by a cluster of two loosely bound valence nucleons orbiting around a ^{9}Li core. In addition, a realistic NN-transition amplitude derived from the Paris interaction [18,19] will also be used in both formalisms. For the purpose of getting insight into the reaction mechanism this is a reasonable approximation even if pion production is not taken into account in the high-energy regimes.

In Sec. II we review the KMT and MST scattering formalisms. In Sec. III we describe the projectile structure model. The results are presented in Sec. IV and discussed in Sec. V.

II. THE MULTIPLE-SCATTERING EXPANSION

For clarity, we briefly describe the few-body multiple scattering expansion of the total transition amplitude and the mean-field multiple-scattering expansion of the optical potential as derived by KMT. Let us consider the scattering of a proton from a nucleus of mass number A, that can be well described as $\mathcal{N}$ weakly bound subsystems, for example ^{11}Li (^{9}Li$+2n$ valence neutrons). Within the MST, the few-body nature of the nucleus is incorporated *ab initio* in the formalism. On the contrary, the mean-field KMT assumes that all the nucleons can be treated on equal footing. It follows that there are two basic underlying differences between the two formalisms.

(1) First, recoil is explicitly taken into account in MST and involves each of the subsystems of the nucleus. In the mean-field KMT the change in momentum of the proton is shared by the nucleus as a whole.

(2) Mean-field OM theories such as KMT assume small contributions to the total transition amplitude from propagation in intermediate excited states. For proton scattering from nuclei with inelastic thresholds close to the ground state, as for example halo nuclei, this assumption is expected to be inadequate. In the case of MST, ground-state and excited-state contributions are implicitly included in a simple way.

Given the same dynamical and structure information, the difference between the calculated differential cross sections can then be traced back to either of these effects.

A. The two-neutron halo-structure input

In both the mean-field KMT and the few-body MST reaction mechanism frameworks, to a good approximation the scattering involves the halo wave function in two distinct ways: First, through the halo density, the probability $\rho_v(\vec{x})$ of finding a valence neutron at a distance $\vec{x}$ from the center of mass of the halo nucleus and, second, through the density distribution for the motion of the core center-of-mass $\rho_{\mathrm{c.m.}}(\vec{x})$. Both of these density functions, in momentum space, are given in terms of the two-body halo density

$$\rho_2(\vec{\Delta}_1,\vec{\Delta}_2)=\int d\vec{Q}_1\, d\vec{Q}_2\, \varphi^*_{nn}(\vec{Q}_1,\vec{Q}_2) \times \varphi_{nn}(\vec{Q}_1+\vec{\Delta}_1,\vec{Q}_2+\vec{\Delta}_2), \tag{1}$$

by

$$\rho_v(\vec{\Delta})=\rho_2\left(\frac{m_3}{M_{23}}\vec{\Delta},\frac{m_4}{M_{234}}\vec{\Delta}\right) \tag{2}$$

and

$$\rho_{\mathrm{c.m.}}(\vec{\Delta})=\rho_2\left(0,\frac{M_{23}}{M_{234}}\vec{\Delta}\right), \tag{3}$$

where $M_{23}=m_2+m_3, M_{234}=m_2+m_3+m_4$. Here, m_2 and m_3 are the masses of the valence neutrons and m_4 the mass of the core. In Eq. (1) $\varphi_{nn}(\vec{Q}_1,\vec{Q}_2)$ is the Fourier transform of wave function of the two-body valence system relative to the core $\varphi_{nn}(\vec{r},\vec{R})$, with $\vec{R}$ and $\vec{r}$ being the core-(nn) and n-n separations, respectively. The departure of $\rho_{\mathrm{c.m.}}(\vec{\Delta})$ from unity arises from core-recoil effects.

B. KMT

The first-order term of the KMT optical potential for nucleon scattering from a nucleus of mass number A is given by the expression [1,16]

$$U=\frac{A-1}{A}\sum_{i=2}^{A+1}\langle\Phi_0|t^f_{1i}(\omega)|\Phi_0\rangle, \tag{4}$$

where the index i runs over all the nucleons in the nucleus. Here, Φ_0 is the nucleus wave function and $t^f_{1i}(\omega)$ is the NN transition operator describing the free-scattering of the incident (1) and struck (i) target nucleon with an energy parameter ω. This transition amplitude satisfies the integral equation

$$t^f_{1i}(\omega)=v_{1i}+v_{1i}g(\omega)t^f_{1i}(\omega), \tag{5}$$

where v_{1i} is the free-space NN interaction. The intermediate-state propagator $g(\omega)$ is

$$g(\omega)=\frac{1}{\omega^+-K_{1i}}, \tag{6}$$

where K_{1i} is the kinetic-energy operator for the relative motion of the interacting NN pair. The energy parameter is taken to be $\omega = E/2$. This assumes that medium effects arising from Pauli blocking, and from distortions due to the struck nucleon binding potential, do not need to be taken into account. These assumptions have been shown, in [16] and [20], respectively, to be good for the case of nucleon scattering at intermediate energy.

The matrix elements of the optical potential are developed in momentum space [9]. For p-^{9}Li scattering, assuming that the ^{9}Li neutrons and the protons have the same matter density distribution,

$$\langle \vec{k}' | U^9 | \vec{k} \rangle = \frac{8}{9} \rho_c(\Delta) \bar{t}_{1c}(\omega, \Delta, Q/2, \phi), \tag{7}$$

with

$$\bar{t}_{1c}(\omega, \Delta, Q/2, \phi) = \frac{6}{9} \bar{t}_{1n}(\omega, \Delta, Q/2, \phi) + \frac{3}{9} \bar{t}_{1p}(\omega, \Delta, Q/2, \phi), \tag{8}$$

where, assuming a spin-zero core, $\bar{t}_{1n}$, $\bar{t}_{1p}$ are the spin averaged pn and pp amplitudes, respectively, and $\rho_c(\Delta)$ is the ^{9}Li matter-density distribution. Here, $\vec{\Delta} = \vec{k}' - \vec{k}$ is the momentum transfer, $\vec{Q} = (\vec{k} + \vec{k}')/2$ is the mean value of the scattered-nucleon momenta, and ϕ is the angle between the vectors $\vec{Q}$ and $\vec{\Delta}$.

For p-^{11}Li scattering,

$$\langle \vec{k}' | U^{11} | \vec{k} \rangle = \frac{10}{11} [\hat{\rho}_c(\Delta) \bar{t}_{1c}(\omega, \Delta, Q/2, \phi) + \rho_v(\Delta) \bar{t}_{1n}(\omega, \Delta, Q/2, \phi)]. \tag{9}$$

The density $\hat{\rho}_c(\Delta)$ is the core density modulated by the density distribution of the core center-of-mass motion $\rho_{\text{c.m.}}(\Delta)$,

$$\hat{\rho}_c(\Delta) = \rho_c(\Delta) \rho_{\text{c.m.}}(\Delta). \tag{10}$$

In the limit of an isospin-independent NN transition amplitude, $\bar{t}_{1n} = \bar{t}_{1p} = \bar{\bar{t}}_{NN}$, so for p-^{9}Li scattering

$$\langle \vec{k}' | U^9 | \vec{k} \rangle = \frac{8}{9} \rho_c(\Delta) \bar{\bar{t}}_{NN}(\omega, \Delta, Q/2, \phi). \tag{11}$$

In the case of p-^{11}Li scattering this limit gives

$$\langle \vec{k}' | U^{11} | \vec{k} \rangle = \frac{10}{11} \rho_{11}(\Delta) \bar{\bar{t}}_{NN}(\omega, \Delta, Q/2, \phi), \tag{12}$$

with $\rho_{11}(\Delta)$ being the total matter-density distribution for ^{11}Li,

$$\rho_{11}(\Delta) = \rho_c(\Delta) \rho_{\text{c.m.}}(\Delta) + \rho_v(\Delta). \tag{13}$$

The scattering observables for p-^{9}Li and p-^{11}Li scatterings are readily evaluated in momentum space in terms of the NA transition amplitude

$$T_{\text{KMT}} = A/(A-1) T(U), \tag{14}$$

where $T(U)$ is the transition operator generated from the optical potential U given by Eqs. (7) and (9).

C. MST

The total transition amplitude T for scattering of a proton from a system composed of a small number $\mathcal{N}$ of subsystems can be written [15]

$$T = \sum_{\mathcal{I}} \hat{t}_{1\mathcal{I}} + \sum_{\mathcal{I}} \hat{t}_{1\mathcal{I}} G_0 \sum_{\mathcal{J} \neq \mathcal{I}} \hat{t}_{1\mathcal{J}} + \cdots, \tag{15}$$

where the proton-$\mathcal{I}$ subsystem transition amplitude satisfies

$$\hat{t}_{1\mathcal{I}} = v_{1\mathcal{I}} + v_{1\mathcal{I}} G_0 \hat{t}_{1\mathcal{I}}. \tag{16}$$

The propagator G_0 contains the kinetic-energy operators of the proton and *all the nuclear subsystems*,

$$G_0 = (E^+ - K)^{-1}. \tag{17}$$

We ignore the interaction between projectile subsystems in G_0 (impulse approximation). Here, k_i is the incident momentum and E the kinetic energy, $E = \hbar^2 k_i^2 / 2\mu_{NA}$ in the overall center-of-mass frame, and μ_{NA} is the proton-projectile reduced mass.

We note that in the MST expansion of the total transition amplitude Eq. (15) *all states*, ground and excited states, are included *implicitly* in the intermediate scattering propagation.

As follows from Eqs. (15)–(17), in the MST expansion the few-body dynamics are properly included, and excitations of the nucleus that involve changes in the relative motion of the subsystems are explicitly taken into account. In the three-body problem of p-d scattering, for example, this means keeping track of the relative motion of deuteron constituents in the folding of the NN transition amplitude with the deuteron ground-state wave function. The core scattering term of Eq. (15), for another example, changes the momenta of the core without changing the neutron states. This necessarily introduces excited states in ^{11}Li as intermediate states during the reaction. In [21] we calculate the explicit cross sections to these excited breakup states, but here these are only *virtual* neutron-halo-breakup states during the *elastic* scattering process.

The contribution to the single-scattering term from proton scattering from one of the valence particles, for example particle 2, is given by

$$\langle \vec{k}_f \Phi | \hat{t}_{12} | \vec{k}_i \Phi \rangle = \langle \vec{k}_f \varphi_{nn} | \hat{t}_{12} | \vec{k}_i \varphi_{nn} \rangle = \hat{t}_{12}(\omega_{12}, \vec{\Delta}) \rho_v(\vec{\Delta}), \tag{18}$$

with the energy parameter ω_{12}

$$\omega_{12} = E \left[1 - \frac{m_1 M_{34}}{M_{12} M_{234}} \right], \tag{19}$$

which reduces to $\omega_{12} = E/2$ in the limit of $m_4 \gg m_3, m_2$.

The contribution to the single-scattering term from proton scattering from the core is

$$\langle \vec{k}_f \Phi | \hat{t}_{14} | \vec{k}_i \Phi \rangle = \langle \varphi_{\rm core} | \hat{t}_{14}(\omega_{14}, \vec{\Delta}) | \varphi_{\rm core} \rangle \rho_{\rm c.m.}(\vec{\Delta}), \tag{20}$$

and the energy parameter ω_{14} given by

$$\omega_{14} = E\left[1 - \frac{m_1 M_{23}}{M_{14} M_{234}}\right]. \tag{21}$$

In the limit of $m_4 \gg 1$, $\omega_{14} = E$.

The contribution of the valence-valence double-scattering term that probes correlation among the valence nucleons was found negligible [15]. The valence-core double-scattering term was found to be

$$\begin{aligned}\langle \vec{k}_f \Phi | \hat{t}_{12} G_1 \hat{t}_{14} | \vec{k}_i \Phi \rangle = & \int d\vec{q}\, \hat{t}_{12}\left(\omega_{12}, \frac{M_{23}}{M_{234}}\vec{\Delta} + \vec{q}\right) \\ & \times \left\langle \varphi_{\rm core} \left| \hat{t}_{41}\left(\omega_{14}, \frac{m_4}{M_{234}}\vec{\Delta} - \vec{q}\right) \right| \varphi_{\rm core} \right\rangle \\ & \times G_1(\vec{q}) \rho_2\left(\frac{m_3}{M_{23}}\vec{q} + \frac{m_3}{M_{234}}\vec{\Delta}, \vec{q}\right), \end{aligned} \tag{22}$$

where

$$G_1(\vec{q}) = 2\frac{\mu_{1(234)}}{\hbar^2}\left[k_i^2 - \left(\frac{(m_4 \vec{k}_f + m_{23}\vec{k}_i)}{M_{234}} + \vec{q}\right)^2 + i\epsilon\right]^{-1}. \tag{23}$$

In addition, we have shown in [15] that, to a good approximation, the two-body halo density in Eq. (22) can be replaced by the halo-density distribution $\rho_v(\vec{\Delta})$,

$$\begin{aligned}\langle \vec{k}_f \Phi | \hat{t}_{12} G_1 \hat{t}_{14} | \vec{k}_i \Phi \rangle = & \int d\vec{q}\, \hat{t}_{12}\left(\omega_{12}, \frac{M_{23}}{M_{234}}\vec{\Delta} + \vec{q}\right) \\ & \times \left\langle \varphi_{\rm core} \left| \hat{t}_{41}\left(\omega_{14}, \frac{m_4}{M_{234}}\vec{\Delta} - \vec{q}\right) \right| \varphi_{\rm core} \right\rangle \\ & \times G_1(\vec{q}) \rho_v(\vec{q}). \end{aligned} \tag{24}$$

Collecting results, to second order in the multiple-scattering expansion,

$$\begin{aligned} T = & \hat{t}_{12}(\omega_{12}, \vec{\Delta}) \rho_v(\vec{\Delta}) + \langle \varphi_{\rm core} | \hat{t}_{14}(\omega_{14}, \vec{\Delta}) | \varphi_{\rm core} \rangle \rho_{\rm c.m.}(\vec{\Delta}) \\ & + \int d\vec{q}\, \hat{t}_{12}\left(\omega_{12}, \frac{M_{23}}{M_{234}}\vec{\Delta} + \vec{q}\right) \\ & \times \left\langle \varphi_{\rm core} \left| \hat{t}_{41}\left(\omega_{14}, \frac{m_4}{M_{234}}\vec{\Delta} - \vec{q}\right) \right| \varphi_{\rm core} \right\rangle G_1(\vec{q}) \rho_v(\vec{q}), \end{aligned} \tag{25}$$

which shows that the relevant halo structure is contained solely in the density distributions ρ_v and $\rho_{\rm c.m.}$. The elastic-scattering observables can then be derived to a good approximation from Eq. (25).

D. Reaction dynamics-structure interplay

As shown in the previous section, the scattering essentially involves the halo wave function in two distinct ways: through the halo density $\rho_v(\Delta)$ of Eq. (2), and the density distribution for the motion of the core center of mass $\rho_{\rm c.m.}(\Delta)$ of Eq. (3).

However, this structure information is combined with the dynamics of the scattering in a different way in the cases of the mean-field and few-body scattering formalism approach. In the first place, the difference between the two frameworks arises even at the level of the first-order term of the few-body MST expansion. Within KMT, and in the limit of an isospin-independent transition amplitude, the structure information appears through the total matter *density* given by the sum of the valence density and a core density modulated by the density distribution of the core center-of-mass motion $\rho_{\rm c.m.}$, Eq. (12). In the MST, Eq. (25), it is the proton-core transition *amplitude* that is modulated in this way. This core-recoil effect can only be neglected in the heavy core limit, when $\rho_{\rm c.m.} = 1$. It was shown, however, in [15] that neglecting these core c.m. effects is a poor approximation in the case considered here. Second, the center-of-mass corrections to the second-order terms do not have in the MST formalism the structure that would arise from iterating the single-scattering approximation of the optical-model KMT theory.

Even when neglecting the isospin independence of the *NN* transition amplitude, the two formalisms can only be made identical if the valence halo nucleons can be treated on an equal footing to the nucleons in the core, and all nucleons assumed to follow the same fraction of the total density. The explicit few-body treatment of the halo nucleus, taken into account within the MST framework, incorporates new physics: core recoil and $2n$ valence breakup. In our calculations, we found that the isospin dependence of the transition amplitude is not too strong at this energy. It is the aim of this work to clarify the role of valence and recoil contributions to the scattering.

III. STRUCTURE MODELS

Realistic structure models for ^{9}Li [10] and for ^{11}Li, within a core$+2n$ valence description [11] have been used in describing proton-lithium scattering [9,10]. Since our aim here is to compare the MF optical-model KMT and few-body MST scattering framework within a consistent structure and with the same *NN* dynamical information, we are not aiming for a detailed comparison with experimental data. So, we shall use simplified structure models, for both ^{11}Li and ^{9}Li nuclei.

A. ^{9}Li structure model

In describing the ^{9}Li ground state we consider a structure model of a Gaussian distribution with a range α_c chosen to reproduce the rms radius of ^{9}Li,

$$\rho_c(\Delta) = 9 \exp(-\alpha_c^2 \Delta^2/4). \tag{26}$$

For $\langle r^2 \rangle_9^{1/2} = 2.32$ fm, then $\alpha_c = 1.89$ fm.

B. The ^{11}Li binary cluster-structure model

We consider the ^{11}Li ground state to be described by a simple structure model [17] of finite-sized core and $2n$ valence clusters. Following the work of [17], the internal densities of the core ρ_c and of the $2n$ valence pair ρ_v are written as single Gaussian functions. In momentum space we represent the Gaussian function with a range parameter γ as

$$g^{(3)}(\gamma,\Delta)=\exp(-\Delta^2\gamma^2/4), \quad \langle r^2\rangle=3\gamma^2/2. \tag{27}$$

The relative-motion wave function of the two clusters, valence and core, is taken as a $0s$ oscillator state of range parameter α related with the mean-cluster separation by $\langle r^2\rangle=3\alpha^2/2$. The total density of the composite nucleus, in the present case ^{11}Li, is then given by $\rho_t(\Delta)=\hat{\rho}_c(\Delta)+\rho_v(\Delta)$, where the halo-valence-cluster density is

$$\rho_v(\Delta)=A_v g^{(3)}(\hat{\alpha}_v,\Delta), \tag{28}$$

and the modulated core-density distribution

$$\hat{\rho}_c(\Delta)=A_c g^{(3)}(\hat{\alpha}_c,\Delta). \tag{29}$$

The range parameters,

$$\hat{\alpha}_v^2=\alpha_v^2+\left(\frac{A_c\alpha}{A_v+A_c}\right)^2, \quad \hat{\alpha}_c^2=\alpha_c^2+\left(\frac{A_v\alpha}{A_v+A_c}\right)^2, \tag{30}$$

are related to the mean-squared radius of the composite nucleus $\langle r^2\rangle$ through

$$\langle r^2\rangle=(3/2)(A_v\hat{\alpha}_v^2+A_c\hat{\alpha}_c^2). \tag{31}$$

According to this cluster model, the density distribution for the motion of the core $\rho_{\text{c.m.}}(\Delta)$ is given by

$$\rho_{\text{c.m.}}(\Delta)=g^{(3)}(\hat{\alpha}_c,\Delta)/g^{(3)}(\alpha_c,\Delta). \tag{32}$$

We fix the radius and thus the range α_c of the core. We also fix the radius of the halo nucleus [Eq. (31)]. For a given cluster separation α, we obtain from Eqs. (30) and (31) the ranges of the valence-density distribution, $\rho_v(\Delta)$, and the modulated core-density distribution $\hat{\rho}_c(\Delta)$. This enables us to construct the total [Eq. (13)] and density distribution for the core center of mass, $\rho_{\text{c.m.}}(\Delta)$ [Eq. (32)]. The effect of including the density distribution for the core center-of-mass motion on the calculated observables can be studied by substituting the momentum distribution given by Eq. (32) by its zero range limit, that is by taking $\rho_{\text{c.m.}}(\Delta)=1$ in the KMT [Eq. (10)], or in the MST framework [Eq. (25)]. In the limit of $\alpha=0$, then necessarily $\rho_{\text{c.m.}}(\Delta)=1$. To reproduce reasonably the realistic few-body wave functions of [12] we chose the parameter $\alpha=4.57$ fm.

IV. RESULTS

The differential elastic-scattering cross section was evaluated making use of the two reaction-scattering frameworks, MST and KMT. For simplicity, only the central parts of the transition amplitudes were considered, and these were assumed to be local [18]. The NN transition amplitude was derived from the Paris potential [18,19]. We also neglect the Coulomb interaction, as this only affects the elastic cross sections at very forward angles. The first- and second-order terms of the MST were evaluated using a NN-transition amplitude at the appropriate fixed-energy parameter with finite mass effects properly taken into account. The transition amplitude for proton scattering from ^{9}Li was generated by the optical potential calculated in the single-scattering approximation [Eqs. (7) and (14)]. In the evaluation of the second-order terms in Eq. (25), the propagators were evaluated using the eikonal approximation and for simplicity the principal value term was neglected.

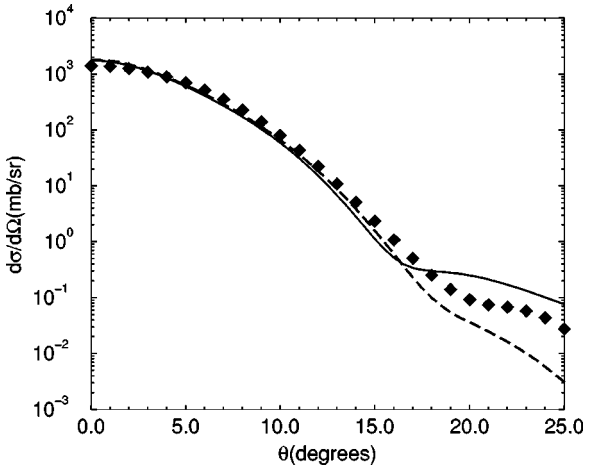

FIG. 1. Calculated differential cross sections for p-^{11}Li scattering at 800 MeV/nucleon. The dashed line includes the single-scattering contribution to MST and the solid line includes the double-scattering corrections. The diamonds represent the KMT results.

The calculated differential cross sections for p-^{11}Li nuclear scattering at 800 MeV/nucleon using the KMT and MST formalisms are presented in Fig. 1. The dashed line uses the single-scattering term of the MST only, and the solid line includes the double-scattering contributions. The KMT results, represented by the diamonds, are significantly different from the MST predictions and show that, while the structure input is the same, there is a different interplay between the structure and reaction formalism at medium and large angles. The double-scattering contribution to the scattering is only important for large momentum transfers, and it needs to be taken into account to have a full understanding of the scattering at these momentum transfers.

As we have shown in Sec. II, the two scattering frameworks handle in different ways recoil and the contributions from intermediate scattering. To disentangle the contributions of the scattering from the valence nucleons and core recoil in both formalisms, we next compare the predictions to the elastic-scattering observables from the KMT and the single-scattering approximation to the MST, when just one or the other of these contributions is taken into account.

In Fig. 2 the differential cross section was evaluated neglecting the contribution of the valence halo neutrons to the scattering and taking $\rho_{\text{c.m.}}=1$ in Eqs. (10) and (25). The diamonds represent the KMT predictions. The dashed line represents the prediction of MST when only the single-

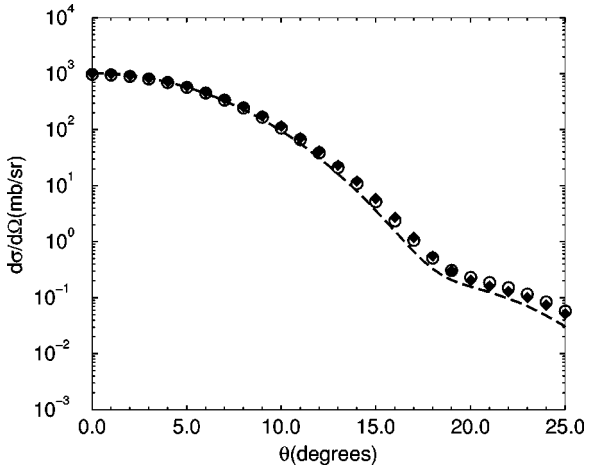

FIG. 2. Calculated differential cross sections for p-^{11}Li scattering at 800 MeV/nucleon using the KMT (diamonds) and single-scattering MST (dashed curve) with $\rho_{\text{c.m.}}=1$ and no valence nucleons. The circles represent the predictions of KMT when the mass factors, in the total transition amplitude and in the optical potential, are taken to unity.

scattering terms are included. The circles show that taking the KMT mass factor in Eqs. (9) and (14) to unity has a negligible effect on the calculated differential cross section. The difference between the predictions of two formalisms are very small in this case and arise because a given momentum transfer corresponds to different scattering angles for different mass targets.

Figure 3 shows the elastic-scattering observable evaluated with $\rho_{\text{c.m.}}=1$ but including the contribution of the valence nucleons to the scattering. In this case the difference between the results from KMT (diamonds) and the single-scattering approximation of the MST approach (dashed line) is relatively small.

On the other hand, if we do not take $\rho_{\text{c.m.}}$ equal to one but still neglect the contribution of the valence nucleons to the

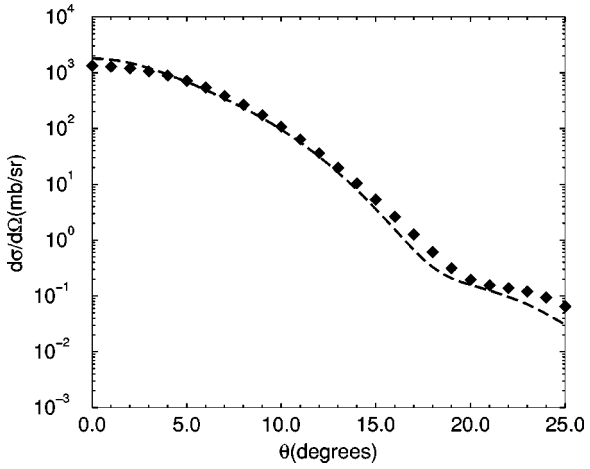

FIG. 3. Calculated differential cross sections for p-^{11}Li scattering at 800 MeV/nucleon using the KMT (diamonds) and single-scattering MST (dashed curve) with $\rho_{\text{c.m.}}=1$ and with valence neutrons.

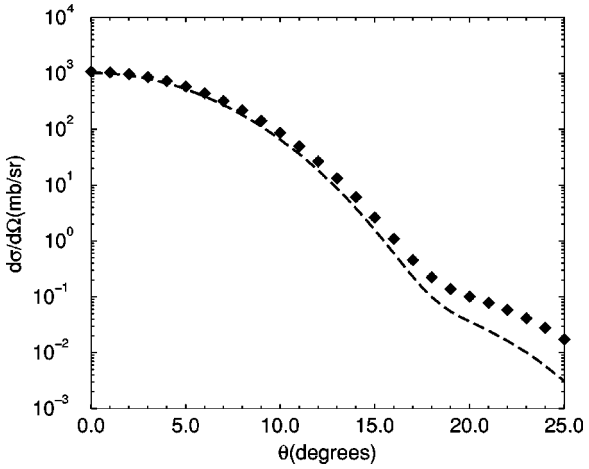

FIG. 4. Calculated differential cross sections for p-^{11}Li scattering at 800 MeV/nucleon using the KMT (diamonds) and single-scattering MST (dashed curve) with no valence nucleons but including core recoil.

scattering, as shown in Fig. 4, the predictions of the different formalisms are significantly different due to core recoil, which is not properly taken into account in a mean-field optical-model theory such as KMT.

To disentangle the contribution of core recoil and the valence nucleons to the scattering in the case of the mean-field KMT and few-body MST, we evaluate the differential cross section setting to zero the mean-cluster separation, $\alpha=0$. In this case, the momentum-space-density distribution for the motion of the core becomes unity, $\rho_{\text{c.m.}}(\Delta)=1$. Reference [17] shows that in this case the predictions of the few-body Glauber formalism are identical to the optical model limit. Figure 5 shows that the KMT results represented by the diamonds approximate, as expected, the single-scattering approximation of the MST (dashed curve). However, the inclusion of the double-scattering contributions (solid line) makes

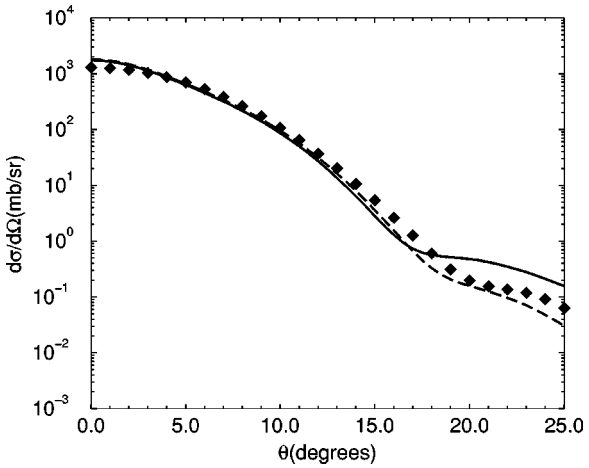

FIG. 5. Calculated differential cross sections for p-^{11}Li scattering at 800 MeV/nucleon taking $\alpha=0$. The dashed line includes the single-scattering contribution to MST and the solid line includes the double-scattering corrections. The diamonds represent the KMT results.

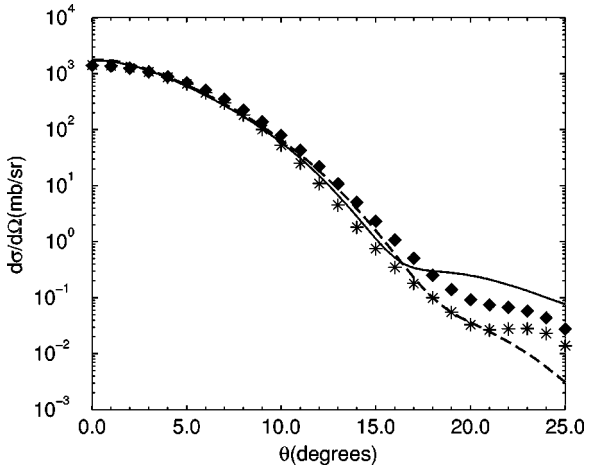

FIG. 6. Calculated differential cross sections for p-^{11}Li scattering at 800 MeV/nucleon using the KMT represented by the diamonds. The stars were obtained from increasing the rms radius of ^{9}Li and ^{11}Li. The dashed line includes the single-scattering contribution to MST and the solid line includes the double-scattering corrections corresponding to the smaller radii case.

the predictions from the two formalisms differ even when we take $\alpha=0$. This is because the two theories differ not only due to the treatment of recoil, but also because the double-scattering contribution of the transition amplitudes includes, within MST, both ground-state and excited-state contributions. For nuclei such as ^{11}Li with inelastic-scattering thresholds close to the ground state, these are expected to be important. The coupling of the elastic with the 2-n halo virtual breakup appears to be important in this case.

To illustrate in which way a variation of the rms radius of the nucleus modifies the differential cross section, we compare in Fig. 6 the KMT results when both the rms radius for the ^{9}Li core, $\langle r^2\rangle_{^9\mathrm{Li}}$ and ^{11}Li $\langle r^2\rangle_{^{11}\mathrm{Li}}$, are increased from 2.39 and 3.39, respectively (diamonds), to 2.8 fm and 3.4 fm (stars), with α kept constant. The dashed line represents the single-scattering approximation for MST and the solid line includes the double-scattering contribution corresponding to the smaller radii case. When the sizes of the cluster systems increase, the calculated KMT differential cross section approaches the single-scattering approximation of the calculated few-body result but deviates from the double-scattering contribution. In other words, core recoil and 2-n halo virtual breakup induce opposite effects onto the differential cross section, and both need to be properly taken into account in order to extract reliable information.

V. CONCLUSIONS

We have explored the effects on the reaction observables of the few-body nature of loosely bound light nuclei such as ^{11}Li, assumed to be well described by two loosely bound valence nucleons orbiting around a ^{9}Li core.

We have evaluated the differential cross section for ^{11}Li scattering from protons at 800 MeV/nucleon using two distinct reaction mechanisms: a mean-field multiple-scattering expansion of the optical potential as derived by KMT, and a few-body multiple-scattering expansion of the total transition amplitude to second order on the transition amplitude for proton scattering from each subsystem. The MST expansion includes explicitly core recoil, and ground state as well as all excited-state contributions in the intermediate scattering for the total transition amplitude. In this case, the contribution from the intermediate states where the valence nucleons' breakup into the continuum are automatically taken into account. The contribution from these excited states to the scattering is assumed to be small with the mean-field KMT framework.

The calculations were performed using the same NN dynamical input and the same densities, namely the halo density and core center-of-mass motion density distributions. We have shown that the mean-field KMT produces significantly different results from the few-body MST. Within the few-body framework *both* (i) core recoil and (ii) contributions due to 2-n halo virtual breakup are taken into account, and these effects were found to produce significant effects in the calculated elastic-scattering data for p-^{11}Li at 800 MeV.

ACKNOWLEDGMENTS

The authors would like to thank Professor R. Johnson for useful discussions. This work was supported by Fundação para a Ciência e Tecnologia (Portugal) through Grant No. Praxis/XXI/PCEX/P/FIS/4/96, and by EPSRC(UK) through Grant No. GR/J95867.

[1] A. K. Kerman, H. McManus, and R. M. Thaler, Ann. Phys. (N.Y.) **8**, 551 (1959).
[2] K. M. Watson, Phys. Rev. **105**, 1338 (1957); M. L. Goldberger and K. M. Watson, *Collision Theory* (Wiley, New York, 1964).
[3] F. A. Brieva and J. R. Rook, Nucl. Phys. **A281**, 317 (1972); J. P. Jeukenne, A. Lejeunne, and C. Mahaux, Phys. Rep., Phys. Lett. **25**, 83 (1976).
[4] G. D. Alkhazov, S. L. Belostotsky, and A. A. Vorobyov, Phys. Rep., Phys. Lett. **42**, 89 (1978).
[5] G. D. Alkhazov *et al.*, Phys. Rev. Lett. **78**, 2313 (1997).
[6] R. Crespo, J. A. Tostevin, and R. C. Johnson, Phys. Rev. C **51**, 3283 (1995).
[7] S. Karataglidis, P. J. Dortmans, K. Amos, and C. Bennhold, Phys. Rev. C **61**, 024319 (2000).
[8] S. P. Weppner, Ofir Garcia, and Ch. Elster, Phys. Rev. C **61**, 044601 (2000).
[9] R. Crespo, J. A. Tostevin, and I. J. Thompson, Phys. Rev. C **54**, 1867 (1996).
[10] S. Karataglidis, P. G. Hansen, B. A. Brown, K. Amos, and P. J. Dortmans, Phys. Rev. Lett. **79**, 1447 (1997).
[11] M. V. Zhukov, D. V. Fedorov, B. V. Danilin, J. S. Vaagen, J. M. Bang, and I. J. Thompson, Nucl. Phys. **A552**, 353 (1993).
[12] J. S. Al-Khalili, J. A. Tostevin, and I. J. Thompson, Phys. Rev. C **54**, 1843 (1996).

[13] J. S. Al-Khalili and J. A. Tostevin, Phys. Rev. C **57**, 1846 (1998).
[14] R. C. Johnson, J. Al-Khalili, and J. A. Tostevin, Phys. Rev. Lett. **79**, 2771 (1997).
[15] R. Crespo and R. C. Johnson, Phys. Rev. C **60**, 034007 (1999); R. Crespo, Nucl. Phys. A (to be published).
[16] R. Crespo, R. C. Johnson, and J. A. Tostevin, Phys. Rev. C **44**, R1735 (1991); **46**, 279 (1992).
[17] J. A. Tostevin, R. C. Johnson, and J. S. Al-Khalili, Nucl. Phys. **A630**, 340c (1998).
[18] E. F. Redish and K. Stricker-Bauer, Phys. Rev. C **36**, 513 (1987).
[19] M. Lacombe, B. Loiseau, J. M. Richard, R. Vinh Mau, J. Côté, P. Pires, and R. de Tourreil, Phys. Rev. C **21**, 861 (1980).
[20] R. Crespo, R. C. Johnson, and J. A. Tostevin, Phys. Rev. C **48**, 351 (1993).
[21] R. Crespo and I. J. Thompson, Nucl. Phys. A (to be published).